Communication

Organized Formation of 2D Extended Covalent Organic Frameworks at Surfaces

Nikolas A. A. Zwaneveld, Re#my Pawlak, Mathieu Abel, Daniel Catalin, Didier Gigmes, Denis Bertin, and Louis Porte

J. Am. Chem. Soc., **2008**, 130 (21), 6678-6679 • DOI: 10.1021/ja800906f • Publication Date (Web): 30 April 2008

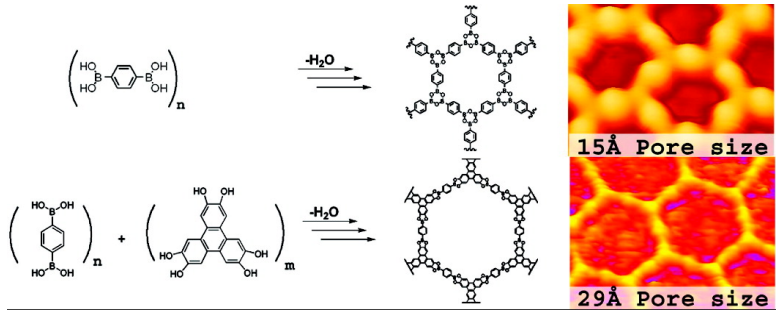

More About This Article

Additional resources and features associated with this article are available within the HTML version:

- Supporting Information
- Links to the 4 articles that cite this article, as of the time of this article download
- Access to high resolution figures
- Links to articles and content related to this article
- Copyright permission to reproduce figures and/or text from this article

View the Full Text HTML

J|A|C|S
COMMUNICATIONS

Published on Web 04/30/2008

Organized Formation of 2D Extended Covalent Organic Frameworks at Surfaces

Nikolas A. A. Zwaneveld,[†] Rémy Pawlak,[‡] Mathieu Abel,*[,‡] Daniel Catalin,[‡] Didier Gigmes,[†] Denis Bertin,[†] and Louis Porte[‡]

Laboratoire Chimie Provence, Faculté des Sciences et Techniques, Universités Aix-Marseille I, II, III-CNRS UMR 6264, Equipe CROPS, campus Saint Jérôme Case 542, 13397 Marseille Cedex 20, France, and Institut Matériaux, Microélectronique et Nanosciences de Provence, Faculté des Sciences et Techniques, Aix-Marseille Université, CNRS UMR 6242, campus Saint Jérôme Case 142, 13397 Marseille Cedex 20, France

Received February 5, 2008; E-mail: mathieu.abel@l2mp.fr

The use of self-organized two-dimensional molecular networks to pattern molecular arrays is currently one of the most promising methods to produce semiconducting architectures beyond what is fundamentally possible with lithography.[1] The production of chemical arrays on the nanometer scale has been achieved to date using hydrogen bonding[2] and metal−organic interactions.[3] However, because of the weak nature of these noncovalent (supramolecular) chemistries,[4] the networks lack the necessary stability to be used for the patterning of many nanotechnological devices.[5] By contrast, covalently bonded systems show higher stability but are more difficult to control, and only a small number of studies exist. These covalent systems include boron−nitride nanomeshes,[6] STM tip-induced polymerization,[7] electropolymerization of thiophenes,[8] and, more recently, the first example of 2D surface polymerization of porphyrins across small ∼10 nm domains.[9]

Herein we show the first example of surface covalent organic frameworks (SCOFs) extended to near-complete monolayer coverage with a tunable nanoporous structure and the stability for further applications. To accomplish this, we use a boronate-based chemistry applied to two-dimensional network formation on metallic surfaces that has previously been shown to be effective for the synthesis of highly ordered three-dimensional covalent organic frameworks (COF).[10]

The versatility of SCOFs was demonstrated by the production of two boronate-based covalently bonded nanoporous surface networks. The first SCOF-1 (see Figure 1b) is obtained by the molecular dehydration of 1,4-benzenediboronic acid (BDBA), with three boronic acid molecules reacting to form a six-membered B_3O_3 (boroxine) ring with the elimination of water. The second SCOF-2 network is formed by the condensation reaction of BDBA and 2,3,6,7,10,11-hexahydroxytriphenylene (HHTP) from an analogous esterification reaction between the boronic acid and the diol groups to form a dioxaborole heterocycle (see Figure 2). The most energetically favorable structure for both the SCOF-1 and SCOF-2 networks is to form a perfect hexagonal array with boroxine or triphenylene moieties at the junctions. The boronate-based chemistry is particularly suited to this application because it largely produces planar molecules.[11]

The molecular arrays were obtained by sublimation of BDBA and HHTP under ultrahigh vacuum (UHV) from two heated molybdenum crucible evaporators onto a clean Ag(111) surface. Imaging of molecular layers was conducted using scanning tunneling microscopy (STM) at room temperature. Full experimental conditions can be seen in the Supporting Information. It should be noted that similar BDBA fluxes were obtained with crucible temperatures in the range of 370 to 460 K because polymerization of BDBA occurred in the crucible, decreasing the quantity of free BDBA over time. We investigated the effect of evaporator and substrate temperatures (300−500 K) during deposition as well as the effect of annealing (up to 770 K) on the formation of the SCOFs. This allowed us to obtain ordered SCOFs with a surface coverage from <1% up to a near entire monolayer. A covalent network was produced even if the substrate was held at room temperature, implying that the reaction activation temperature is below this. The quality of the network was largely unaffected by changes in the experimental parameters. The only visible effect is the removal of impurities and/or water molecules produced during the polymerization process.

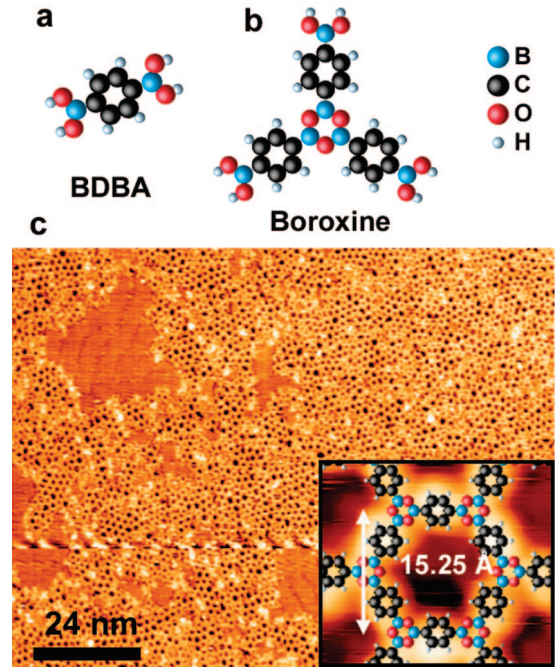

Figure 1. SCOF-1 formed from BDBA deposition on Ag(111): (a) the chemical structure of BDBA; (b) the chemical structure of the boroxine repeat unit formed from dehydration of 3 BDBA monomers; (c) STM image (120 nm × 90 nm) of near-complete monolayer SCOF-1 film. The tunneling conditions were $I = 0.4$ nA, $V = -2.1$ V. The inset shows the overlaid chemical structure obtained by DFT calculation.

Figure 1 shows STM images of the SCOF-1 organized nanoporous molecular film extended over the surface. The measured first neighbor distance between pores was 15 ± 1 Å, which is in good agreement with the 15.25 Å size predicted using density functional

[†] Laboratoire Chimie Provence.
[‡] Institut Matériaux, Microélectronique et Nanosciences de Provence.

10.1021/ja800906f CCC: $40.75

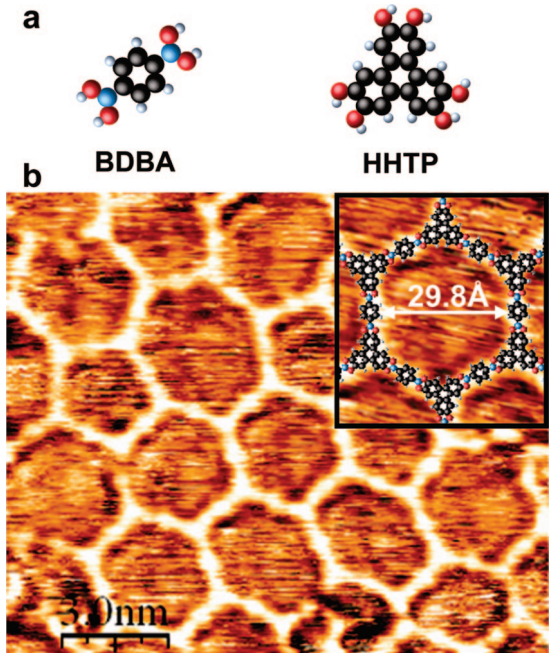

Figure 2. SCOF-2 formed from BDBA and HHTP on Ag(111). (a) Chemical structure of BDBA and HHTP molecules; (b) STM image of the SCOF-2 network showing hexagonal and other polygon structures (e.g., pentagons and heptagons). The tunneling conditions were $I = 1.7$ nA, $V = -2.2$ V. The inset shows the SCOF-2 network with overlaid chemical structure obtained by DFT calculation.

theory (DFT)[12] (see Figure 1c) and thus confirms the covalent formation of the boroxine-linked SCOF-1. The very high thermal stability of the SCOF-1 was demonstrated by annealing the sample up to 750 K for 5 min without degradation. However, after extended periods (12 h at 750 K), significant degradation was noted and only small domains of intact SCOF-1 remain visible. This can be compared to the polymer degradation temperature of 762 K obtained from thermal gravimetric analysis (see Supporting Information).

The surface is composed of a network of polygons, which is dominated by hexagons, but other structures can be found such as five-, seven-, and eight-membered rings. With careful observation, it can be seen that the different polygon structures are caused by either deformation of the perfect hexagon structure or an incomplete ring closure in the boroxine. Overall, the observed polygon distribution results from only a small number of faults in the covalent bond formation. Annealing of the network to remove these faults was ineffective, further confirming the permanent nature of the bonding in the network.

One of the great advantages of SCOFs is the ability to control the size and chemical functionality of the network by the use of two complementary molecular building blocks, in this case, BDBA and HHTP. To inhibit the homopolymerization of BDBA, a monolayer of HHTP was initially deposited, followed by co-deposition of the two molecules. Excess HHTP and water produced during polymerization were then removed from the surface by annealing.

The co-deposition of HHTP and BDBA produced the larger 29 Å SCOF-2 nanoporous array shown in Figure 2b, which is in very good agreement with the theoretical 29.8 Å pore size obtained from DFT calculations.[12] The network is again dominated by hexagonal structures with some defects present in the film. As with SCOF-1, annealing of the sample up to 750 K did not degrade the structure of the network, confirming the covalent nature of the molecular network.

The comparison between the SCOF-1 and SCOF-2 shows that the latter produces a network with fewer defects on the local level. This is likely because the dioxaborole formation reaction is a bimolecular reaction as opposed to the trimolecular boroxine reaction, thus follows a more favorable kinetic path. Other effects such as the increased rigidity of the triphenylene group and the dilution effect of adding the HHTP molecule may also play a part in this improvement.

Thus, our work has demonstrated the ability to form surface covalent organic frameworks of varying pore sizes. This is the first example of such a network exhibiting an extended array over such a large area and the high temperature stability to conduct further functionalization. These properties are essential for further application in the patterning of nanoscopic arrays of magnetic, catalytic, or electronic devices.

Acknowledgment. This work was supported by the "Agence Nationale de la Recherche" under Grant PNANO 06-0251.

Supporting Information Available: Complete experimental procedures, STM images, TGA spectra, chemical mechanisms, and computational details. This material is available free of charge via the Internet at http://pubs.acs.org.

References

(1) (a) Ito, T.; Okazaki, S. *Nature* **2000**, *406*, 1027–1031. (b) Joachim, C.; Gimzewski, J. K.; Aviram, A. *Nature* **2000**, *408*, 541–548.
(2) (a) Theobald, J. A.; Oxtoby, N. S.; Phillips, M. A.; Champness, N. R.; Beton, P. H. *Nature* **2003**, *424*, 1029–1031. (b) Spillmann, H.; Kiebele, A.; Stohr, M.; Jung, T. A.; Bonifazi, D.; Cheng, F. Y.; Diederich, F. *Adv. Mater.* **2006**, *18*, 275. (c) Stohr, M.; Wahl, M.; Galka, C. H.; Riehm, T.; Jung, T. A.; Gade, L. H. *Angew. Chem., Int. Ed.* **2005**, *44*, 7394–7398. (d) De Feyter, S.; De Schryver, F. C. *Chem. Soc. Rev.* **2003**, *32*, 393–393.
(3) (a) Stepanow, S.; Lingenfelder, M.; Dmitriev, A.; Spillmann, H.; Delvigne, E.; Lin, N.; Deng, X. B.; Cai, C. Z.; Barth, J. V.; Kern, K. *Nat. Mater.* **2004**, *3*, 229–233. (b) Schlickum, U.; Decker, R.; Klappenberger, F.; Zoppellaro, G.; Klyatskaya, S.; Ruben, M.; Silanes, I.; Arnau, A.; Kern, K.; Brune, H. *Nano Lett.* **2007**, *7*, 3813–3817. (c) Lin, N.; Stepanow, S.; Vidal, F.; Kern, K.; Alam, M. S.; Stromsdorfer, S.; Dremov, V.; Muller, P.; Landa, A.; Ruben, M. *Dalton Trans.* **2006**, 2794–2800.
(4) (a) Whitesides, G. M.; Grzybowski, B. *Science* **2002**, *295*, 2418–2421. (b) Lehn, J. M. *Science* **1993**, *260*, 1762–1763. (c) Yokoyama, T.; Yokoyama, S.; Kamikado, T.; Okuno, Y.; Mashiko, S. *Nature* **2001**, *413*, 619–621.
(5) Joo, S. H.; Choi, S. J.; Oh, I.; Kwak, J.; Liu, Z.; Terasaki, O.; Ryoo, R. *Nature* **2001**, *412*, 169–172.
(6) Corso, M.; Auwarter, W.; Muntwiler, M.; Tamai, A.; Greber, T.; Osterwalder, J. *Science* **2004**, *303*, 217–220.
(7) (a) Miura, A.; De Feyter, S.; Abdel-Mottaleb, M. M. S.; Gesquiere, A.; Grim, P. C. M.; Moessner, G.; Sieffert, M.; Klapper, M.; Mullen, K.; De Schryver, F. C. *Langmuir* **2003**, *19*, 6474–6482. (b) Okawa, Y.; Aono, M. *Nature* **2001**, *409*, 683–684. (c) Alvarado, S. F.; Riess, W.; Jandke, M.; Strohriegl, P. *Org. Electron.* **2001**, *2*, 75–82.
(8) Sakaguchi, H.; Matsumura, H.; Gong, H. *Nat. Mater.* **2004**, *3*, 551–557.
(9) Grill, L.; Dyer, M.; Lafferentz, L.; Persson, M.; Peters, M. V.; Hecht, S. *Nature* **2007**, *2*, 687–691.
(10) (a) Cote, A. P.; El-Kaderi, H. M.; Furukawa, H.; Hunt, J. R.; Yaghi, O. M. *J. Am. Chem. Soc.* **2007**, *129*, 12914. (b) El-Kaderi, H. M.; Hunt, J. R.; Mendoza-Cortes, J. L.; Cote, A. P.; Taylor, R. E.; O'Keeffe, M.; Yaghi, O. M. *Science* **2007**, *316*, 268–272. (c) Tilford, R. W.; Gemmill, W. R.; zur Loye, H. C.; Lavigne, J. J. *Chem. Mater.* **2006**, *18*, 5296–5301.
(11) (a) Brock, C. B.; Minton, R. P.; Niedenzu, K. *Cryst. Struct. Commun.* **1987**, *43*, 1775–1779. (b) Zettler, V. F.; Hausen, H. D.; Hess, H. *Acta Crystallogr., Sect. B: Struct. Sci.* **1974**, *30*, 1876–1878.
(12) Calculations are based on the pseudopotential density functional theory implemented in the SIESTA program. It uses generalized gradient approximation described by Perdew-Burke and Ernzerhof, Troullier-Martins pseudopotentials and a basis set of double-ζ augmented by polarization functions (DZP basis set). See Supporting Information.

JA800906F